Reliability of the one-crossing approximation in describing the Mott transition

V. Vildosola

Depto de Física CAC-CNEA and Consejo Nacional de Investigaciones Científicas y Técnicas, CONICET, República Argentina

L. V. Pourovskii

Centre de Physique Théorique, École Polytechnique, CNRS, 91128 Palaiseau, France

L. O. Manuel

Instituto de Física Rosario, Consejo Nacional de Investigaciones Científicas y Técnicas and Universidad Nacional de Rosario, Bvd. 27 de Febrero 210 Bis, 2000 Rosario, República Argentina

P. Roura-Bas

Depto de Física CAC-CNEA and Consejo Nacional de Investigaciones Científicas y Técnicas, CONICET, República Argentina

Abstract.

We assess the reliability of the one-crossing approximation (OCA) approach in quantitative description of the Mott transition in the framework of the dynamical mean field theory (DMFT). The OCA approach has been applied in the conjunction with DMFT to a number of heavy-fermion, actinide, transition metal compounds, and nanoscale systems. However, several recent studies in the framework of impurity models pointed out to serious deficiencies of OCA and raised questions regarding its reliability. Here we consider a single band Hubbard model on the Bethe lattice at finite temperatures and compare the results of OCA to those of a numerically exact quantum Monte Carlo (QMC) method. The temperature-local repulsion U phase diagram for the particle-hole symmetric case obtained by OCA is in good agreement with that of QMC, with the metal-insulator transition captured very well. We find, however, that the insulator to metal transition is shifted to higher values of U and, simultaneously, correlations in the metallic phase are significantly overestimated. This counter-intuitive behavior is due to simultaneous underestimations of the Kondo scale in the metallic phase and the size of the insulating gap. We trace the underestimation of the insulating gap to that of the second moment of the high-frequency expansion of the impurity spectral density. Calculations for the system away from the particle-hole symmetric case are also presented and discussed.

PACS numbers: 73.23.-b, 71.10.Hf, 75.20.Hr

1. Introduction

In the past years, many efforts have been devoted to the implementation of calculation techniques to describe the electronic structure of strongly correlated complex materials. This is a complicated and challenging task in view of the many degrees of freedom involved. One of the most successful approaches in this direction was the implementation of the dynamical-mean field theory (DMFT) [1, 2, 3]. Numerically, the most challenging part of DMFT is the solution of the Anderson impurity model [4] within the DMFT self-consistent loop that maps the lattice problem into a single impurity one.

There are two well-known numerically exact techniques to solve this impurity model, namely, the quantum Monte Carlo (QMC) in its Hirsch-Fye (HF-QMC) or continuous time (CT-QMC) versions [5, 6], and the numerical renormalization group (NRG) [7, 8]. Recently, a substantial technical progress [9] has been achieved in both approaches. On one hand, the advent of continuous-time quantum Monte Carlo methods [10] eliminated the time discretization error, inherent to the HF-QMC, and extended the range of applicability of QMC to much lower temperatures and realistic Coulomb repulsion vertices. On the other hand, very fast implementations of NRG applied to multi-band systems has been developped using Abelian and non-Abelian symmetries on a generic level [11].

In spite of recent technical improvements, those exact methods still encounter certain difficulties. QMC solvers suffer from the well known 'fermion sign problem', which can be especially severe when the degeneracy of the correlated shell is large and significant off-diagonal terms are present in the hybridization function. Moreover, QMC calculations are carried out in the imaginary-time domain and an analytic continuation is required to obtain real-energy spectral functions from QMC data. The NRG approach becomes computationally expensive in multiorbital cases with broken orbital symmetries (for instance, when interactions, like pair-hopping, prohibit the use of symmetries that reduce the size of the matrix to be diagonalized [12], leading to an exponential increase of the Hilbert space). Because of these limitations the necessity to have faster and reliable impurity solvers is evident.

Hence, several approximate schemes have been proposed for solving the DMFT impurity problem, like the local moment approximation (LMA)[13], iterative perturbation theory (IPT)[14], exact diagonalization[15], rotationally invariant slave bosons [16], conserving diagrammatic approximations based on self-consistent hybridization expansion (SCH) [17], among others.

Regarding the SCH, the non-crossing approximation (NCA) [18] represents the simplest family of these self consistent treatments and provides an accurate calculation of the impurity Green function, as well as many other properties, when the Coulomb repulsion is taken to be large enough as compared with the other energy scales involved in the problem. However, when more than one charge fluctuation needs to be included ($N \to N-1$ and $N \to N+1$, being N the impurity valence), NCA has failed to give the correct Kondo scale (T_K). The next leading order in the self consistent expansion,

that partially solves this pathology, is often known as the one-crossing approximation, OCA [19, 20, 21]. Within this extended formalism other classes of problems have been investigated [22, 23, 24]. Among them, its major application is in the context of the dynamical mean field theory as an impurity solver [3].

In particular, the OCA solver has the advantage of being formulated at the real frequency axis and it gives the correct order of magnitude for the Kondo scale of the impurity problem. It successfully captures the correct temperature dependence of transport properties of a single impurity level [21], and it has been employed as the DMFT impurity solver in a search for signatures of a non-Fermi liquid behavior in the Hubbard model with van Hove singularities [24]. Furthermore, it has been generalized to an arbitrary number of orbitals and interactions [23]. Multiorbital generalization of OCA were employed in a study of the itinerant and local-moment magnetism in the three-band Hubbard model [27]. In combination with *ab-initio*+DMFT calculations, the OCA solver has been applied to real strongly correlated materials, for example, to heavy-fermion compounds [3, 23, 25, 22].

However, the OCA solver has also several limitations. It cannot be applied to arbitrary low temperatures due to violations of the Fermi-liquid properties (in the impurity model, OCA works well for $T > 0.1T_K$) [21, 28, 29, 30], and it also violates the sum rules for the coefficients of the high-frequency expansion of the self-energy [31]. While the former pathology can be controlled by restricting its application to high enough temperatures, the later one is intrinsic and will always be present. As has been pointed out recently, the OCA method is more accurate in the strongly-correlated limit [31], and it describes the insulating phase particularly well [32]. It has also been shown that OCA overestimates the correlations in th metallic phase and it has been conjectured that this overestimation of correlation effects reflects the fact that the OCA tends to favor the insulating state.

One important issue that has not been studied up to date is the actual quantitative performance of the OCA solver within DMFT in describing the metal-insulator Mott transition[33]. Hence, we address this issue in the present work by calculating the critical U_c values for the Mott transition within DMFT as a function of temperature using OCA as the impurity solver, and comparing them with the corresponding ones obtained with the CT-QMC. We have also compared the DMFT local self-energies obtained within the two approaches as well as the corresponding quasi-particle effective masses in the metallic phase. Our calculations have been carried out for the single band Hubbard model with a semicircular non-interacting density of states.

Our main conclusion is that the OCA metal-to-insulator transition for the particle-hole symmetric case is in remarkably good agreement with that of CT-QMC. However, we find that insulator-to-metal transition is shifted to higher values of U despite the fact the correlations of the metallic phase are overestimated. This counter-intuitive behaviour is explained as a combination of two factors: the underestimation of the effective Kondo temperature in the metallic phase and the underestimation of the gap in the insulating one. The fact that OCA underestimates the gap in the insulating

regime comes out from an analysis of the high-frequncy expansion sum rules of the Green function. Our results are in contradiction to the conjecture of OCA favoring the insulating phase. We show that although OCA overestimates the strength of correlations in the metallic phase, it does not favor the insulating one because the critical values of the metal-to-insulator transition are very well captured.

We have also study the same model in the non-symmetric case, obtaining similar agreement between both techniques. We verify that the OCA approximation does not violate the Friedel sum rule in the metallic phase for the range of temperatures of the obtained phase diagram, and that the interacting part of the OCA self-energy always remains causal.

The paper is organized as follows: we describe the theoretical formalism in section 2, we present the numerical results for the particle-hole symmetric case in section 3.1, we discuss the results obtained for the system away from half-filling in section 3.2 and finally we conclude in section 4.

2. Model and Formalism

We start with the single-band Hubbard Hamiltonian,

$$H = -\frac{t}{\sqrt{z}} \sum_{<ij>\sigma} (c^{\dagger}_{i\sigma} c_{j\sigma} + c^{\dagger}_{j\sigma} c_{i\sigma}) + U \sum_{i} n_{i\uparrow} n_{i\downarrow}, \tag{1}$$

where the first term is the kinetic energy, t is the hopping between nearest neighbors on a lattice, z is the coordination number, and U is the energy of the on-site Coulomb repulsion. The operator $c^{\dagger}_{i\sigma}$ creates an electron with the spin σ on the site i and $n_{i\sigma} = c^{\dagger}_{i\sigma} c_{i\sigma}$. We use the semicircular non-interacting density of states $N(\omega) = \frac{1}{2\pi t^2}\sqrt{4t^2 - \omega}$, $|\omega| < 2t$ corresponding to a Bethe lattice with coordination $z \to \infty$, for which the DMFT approximation becomes exact. In the following we use the half bandwidth as our unit of energy $D = 2t = 1$.

We solve the Hamiltonian [1] by means of DMFT, which maps the lattice model onto a single-impurity Anderson one within a self-consistent cycle. The hopping between the impurity and the conduction band, V_k, defines the hybridization function for the single-impurity problem $\Gamma(i\omega) = \sum_k V_k^2/(i\omega - \epsilon_k)$, where ϵ_k is the conduction energy of the impurity model. Within the DMFT and in the case of the Bethe lattice, the DMFT hybridization function is given by the self-consistency condition $\Gamma(i\omega) = t^2 G[\Gamma(i\omega)]$, where $G(\omega)$ is the local Green function obtained from the impurity model.

Starting from the metallic non-interacting solution of the model, the system turns into an insulator for large enough values of the Coulomb repulsion U due to the vanishing of the quasiparticle weight. The value of $U = U_{c2}$ defines this transition. On the other hand, starting from an insulating solution, the systems turns metallic due to the collapse of the gap between the Hubbard bands, for $U \leq U_{c1}$, with $U_{c1} < U_{c2}$ when T is lower than the second-order end point of the first-order Mott transition T_c. The critical values $U_{c1} < U < U_{c2}$ as function of the temperature T determine a phase diagram.

The phase diagram of the Mott transition for the present model have been previously obtained using the QMC [34, 35, 36], IPT [1], exact diagonalization [37, 38, 39], and NRG[8] impurity solvers. The determination of the exact boundaries of the coexistence region has previously required a significant effort due to their sensitivity to calculational parameters, as well as due to the critical slowing down of the DMFT convergence close to those boundaries [35]. Hence, we have employed up to 220 DMFT cycles for each point in the $\{U, T\}$ space and used a dense mesh along the U axis with the spacing between U values down to 0.005 in the vicinity of the U_{c1} line. We have used the CT-QMC implementation provided by the TRIQS package [40, 41]. The DMFT impurity problem has been solved by CT-QMC using $\sim 10^9$ CT-QMC moves with each 200 moves followed by a measurement. The resulting CT-QMC phase diagram is in agreement with the extensive HF-QMC calculations of Blümer [36]. Within the OCA solver we have used the procedure described by Hettler *et al.* for regularizing the spectral functions [42] and the numerical convolution sketched in Ref.[22] when computing the self-energies and the Green function.

3. Numerical Results

In this section, we present the numerical results obtained using the OCA solver for the DMFT loop and a detailed comparison with CT-QMC calculations.

3.1. Mott transition for the particle-hole symmetric case

In order to get the critical values $U_{c1}(T)$ and $U_{c2}(T)$ for a given temperature T within the OCA solver, we take advantage of its self-consistent nature building an external loop running in the U values. Starting from a metallic solution we slowly increase U by δU retaining the previous ionic self-energies and Green function as the initial guess for the following $U + \delta U$ DMFT cycle, until an insulator solution is reached, and then we decrease U by $-\delta U$ until we go back to the initial U.

In Fig.[1a] we show the spectral weight at the zero-frequency, $A(\omega = 0) = -\mathcal{I}m[G(\omega = 0)]/\pi$, as a function of U for an inverse temperature $\beta = 80$. We show both the increasing U results from the metallic to insulator solutions as well as the decreasing ones. An hysteresis curve is formed, giving rise to two different critical values, $U_{c1}(T)$ and $U_{c2}(T)$. We define these critical values following the criteria given in Ref.[8], from the U-value for which $|A'(\omega = 0)|$ reaches its maximum intensity.

In Fig.[1b] we show the variation of the quasiparticle weights, $Z = [1 - \frac{\partial Re\Sigma(\omega)}{\partial \omega}|_{\omega=0}]^{-1}$, as a function of U for $\beta = 80$. In order to compared with CT-QMC, we first obtain the interacting part of the OCA self-energy $\Sigma(\omega)$, removing the non-interacting offset given by the hybridization term. Secondly, from a Hilbert transform of $Im\Sigma(\omega)$, we compute the corresponding self-energy in the Matsubara domain,

$$\Sigma(i\omega_n) = -\frac{1}{\pi}\int d\omega \, \frac{Im\Sigma(\omega)}{i\omega_n - \omega}. \tag{2}$$

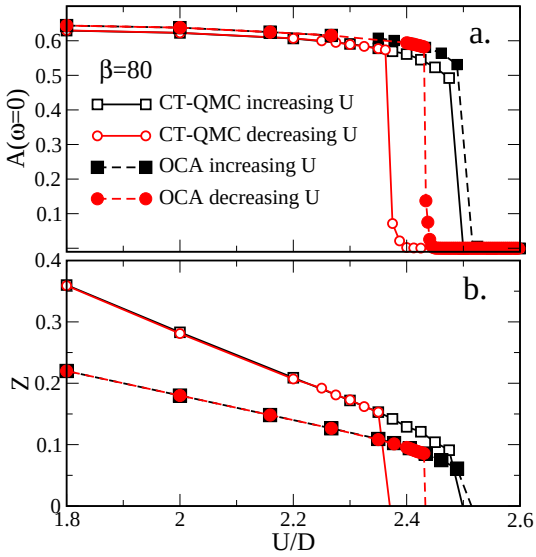

Figure 1. (Color online) a). Spectral weight $A(\omega = 0)$ for the inverse temperature $\beta = 80$ as a function of U both for increasing (black lines, squares) and decreasing (red lines, circles) U values. The CT-QMC (OCA) data are displayed with the solid (dashed) lines and empty (filled) symbols, respectively. b). The quasi-particle residue Z as function of U for the same temperature. The notation is the same as in panel a).

Finally, we approximate the derivative $\frac{\partial Re\Sigma(\omega)}{\partial\omega}|_{\omega=0} = \frac{\partial Im\Sigma(i\omega_n)}{\partial i\omega_n}|_{i\omega_n\to 0}$ by a cubic fitting of the first four Matsubara's frequencies of $Im\Sigma(i\omega_n)$.

Although the vanishing of Z defines the critical value U_c only at zero temperature [8], it has been used as a common criteria even for finite temperatures (see for instance Ref.[43]) From Fig.[1] it can be seen that both approaches (from $A(\omega = 0)$ or from Z) define the same energy scales for U_{c1} and U_{c2}. More importantly, the OCA critical U-values are in a reasonable agreement with the CT-QMC ones. While the OCA value for U_{c2} is obtained within an error of less than 0.5% with respect to the CT-QMC one, the calculated U_{c1} is larger than the CT-QMC one by around 3% . We will discuss the origin of this discrepancy for U_{c1} later in this section.

It is important to remark that the OCA values of Z in the metallic region, i.e. $U < U_{c1}, U_{c2}$, are smaller than the CT-QMC ones. The same behavior was found by Schmitt *et al.* [27] using OCA for a body-centered-cubic lattice in comparison with NRG calculations. While OCA gives the correct low energy scale for the impurity model, this energy scale is still slightly underestimated [20], and therefore within OCA the system feels a larger effective Coulomb repulsion giving rise to a reduced quasiparticle weight. However, it is important to remark that the underestimation of Z is less important close to the transition.

In Fig.(2) we show the imaginary part of the self-energy in the imaginary frequency domain for the increasing U regime at $\beta = 60$ and for two different values of U, one below and one above U_{c_2}, $U = 2.3$ and $U = 2.4$. As it can be observed from this plot, for the metallic case, OCA overestimates the absolute magnitude of the self-energy at

low frequencies. Similarly to the underestimation of the quasiparticle weigth at low temperatures described above, this behavior of $Im\Sigma(i\omega_n)$ can be also understood as arising due to an effectively larger value of U. On the other hand, in the insulating region the agreement between OCA and CT-QMC is remarkable. We found that for a correct comparison between the two techniques it was very important to have the same degree of precision of the convergence criterion of the DMFT loops, especially for points close to the Mott transtion. For large frequencies, an additional test can be done using the sum rules that $\Sigma(i\omega_n)$ should satisfy.

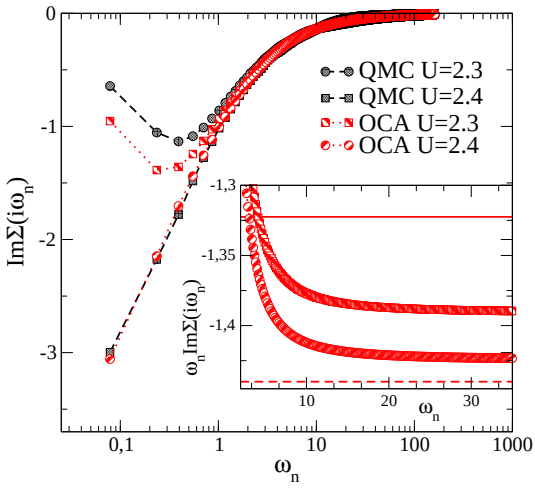

Figure 2. (Color online) Comparison of the imaginary part of the self-energy as a function of the Matsubara frequency between OCA and CT-QMC at $\beta = 60$ for two different values of U, one below the U_{c2} and the other one above. The inset shows the imaginary part of the OCA self-energy scaled by ω_n. The dashed and solid lines indicate their expected theoretical values given by the high frequency expansion sum rule, $\Sigma_1 = -U^2/4$.

In the inset of Fig.(2) we plot the imaginary part of the OCA self-energy scaled by ω_n for $U = 2.3 < U_{c2}$ and $U = 2.4 > U_{c2}$, together with the exact coefficient Σ_1 for each U, that corresponds to the first moment in the self-energy high frequency expansion, $\Sigma_1 = \int \frac{d\omega}{\pi}\, Im\Sigma(\omega)$, and that determines the asymptotic $1/\omega_n$ behavior. In Ref.[31], Rüegg *et al.* have calculated the exact value expected for Σ_1, being $\Sigma_1 = -U^2/4$ for the symmetric case [44]. For the parameters shown in Fig.(2), we obtain a deviation of the OCA Σ_1 coefficient of the order of 5% in the metallic phase, while in the insulator one the error is reduced to less than 2%.

In what follows we discuss the phase diagram of the Mott transition. In Fig.[3] we show the T vs. U diagram with the calculated U_{c_1} and U_{c_2} obtained from the zero-frequency spectral function $A(\omega = 0)$ (upper panel), as well as the quasiparticle residue Z (lower panel). The general trend of the critical $U_c(T)$ obtained by OCA is in reasonable agreement with the corresponding CT-QMC ones. Even though a very well defined coexistence region is captured by OCA, this coexistence region is reduced with respect to the CT-QMC one. While the agreement is remarkable for the $U_{c2}(T)$

transition, the $U_{c1}(T)$ values are slightly shifted to higher energies in OCA.

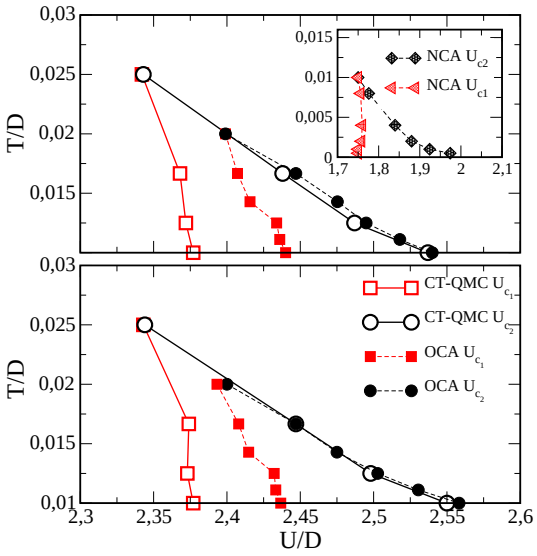

Figure 3. (Color online) The T vs. U phase diagram of the Mott transition obtained from the zero-frequency spectral function $A(\omega = 0)$ (upper panel) and the quasiparticle residue Z (lower panel). The inset in the upper panel indicates the phase diagram obtained using the finite-U NCA in the symmetric case as the impurity solver.

Regarding the critical temperature (T_c) below which two different spinodal lines define the coexistence region of the insulating and metalic regimes of the Mott transition, OCA gives $T_c \sim 0.02$ in reasonable agreement with the CT-QMC $T_c \sim 0.025$. The slight underestimation of T_c is a consequence of the corresponding underestimation of T_K by OCA at the effective impurity level. For comparison, we also include in the inset of the upper panel of Fig.[3] the finite-U NCA phase diagram for the particle-hole symmetric case. We stress here that this simple approximation severely underestimates all the energy scales involved, T_c and both $U_{c1}(T)$ and $U_{c2}(T)$, as a consequence of the underestimated Kondo scale. On the other hand, we want to mention here that the IPT results [1, 8] are considerably shifted to higher energies overestimating both, $U_{c1}(T)$ and $U_{c2}(T)$, due to the exaggerated overestimation of the Kondo scale at the impurity level.

Despite its approximate nature, the coexistence region given by OCA is in the correct energy range and the critical temperature T_c is in very good agreement with the CT-QMC results. We want to remark that for the whole range of temperatures studied in the presented phase diagram, the OCA self-energy remains causal, that is, $Im\Sigma(i\omega_n)$ is negative. For very low temperatures ($T \lesssim 1/500 \sim 0.1\ T_c^{OCA}$), it can turn positive signaling the breakdown of the approximation.

We turn now to the discussion regarding the slight overestimation of U_{c1} that can be observed in Fig.(3). While the value of U_{c2} is given by the critical U for which the

quasiparticle weight at zero frequency vanishes, the U_{c1} is related to the corresponding U for which the Hubbard bands collapse and the gap in the spectral function is closed. We found that the size of the gap in the insulator regime given by OCA is somewhat underestimated and therefore it closes for a larger value of U than expected for CT-QMC. This statement follows from an analysis of the high frequency expansion of the local Green function. As described in Ref.[31], the high frequency expansion in the imaginary domain of $G(i\omega_n)$ is given by

$$G(i\omega_n) = \sum_{k=1}^{\infty} \frac{M_{k-1}}{(i\omega_n)^k}, \tag{3}$$

where, in the spectral representation of the Green function, the coefficients are related to the moments of the spectral density as $M_k = \int_{\infty}^{\infty} d\omega\ \omega^k A(\omega)$ ‡ . Exact relations for the coefficients can be found from thermodynamic expectation values [31]: $M_0 = 1$, $M_1 = \epsilon_d + U n_d/2$ (0 at half filling), and $M_2 = \epsilon_d^2 + \Delta_1 + U(2\epsilon_d + U) n_d/2$. Here, ϵ_d and n_d are the energy level and total occupancy of the effective Anderson model. M_0 and M_1 are related to the normalization and parity of $A(\omega)$ so that they are exactly reproduced by OCA.

Regarding the coefficient M_2, the parameter Δ_0 represents the zero moment in the hybridization high frequency expansion, $\Delta_0 = -\frac{1}{\pi}\int_{\infty}^{\infty} d\omega\ \mathcal{I}m\Gamma(\omega) = \frac{1}{\pi}\int_{\infty}^{\infty} d\omega\ \Delta(\omega)$, where $\Delta(\omega) = \pi V^2 \rho_c(\omega)$, and ρ_c is the conduction density of states. Using the self-consistency condition $\Gamma(i\omega) = t^2 G[\Gamma(i\omega)]$ for the present case of the Bethe lattice, we arrive to the following relation: $\Delta(\omega) = \pi t^2 A(\omega) = \frac{\pi D^2}{4} A(\omega)$. Therefore, $\Delta_0 = \frac{D^2}{4}\int_{\infty}^{\infty} d\omega\ A(\omega) = \frac{D^2}{4}$. Taking into account that for the symmetric situation $2\epsilon_d + U = 0$ and $M_1 = 0$, the coefficient M_2 reads

$$M_2 = \frac{U^2}{4} + \frac{D^2}{4}. \tag{4}$$

The second moment M_2 of the spectral function contains indirect information about the size of the Mott gap. In fact, it carries information about the center position and width of each Hubbard band. For instance, in the simplest case in which the Hubbard bands have the semicircular shape centered at $\pm\omega_0$ and width D, the second moment becomes $M_2 = \omega_0^2 + D^2/4$ by comparing with Eq.(4), one can infer that $\omega_0 = U/2$. In this simple picture, the gap is opened when U is larger than $2D$ and the size of the gap is of the order of $\delta = U - 2D$. In Fig.(4), we show the spectral density in the insulating region when decreasing the Coulomb repulsion from $U = 3$ to $U = 2.6$. It can be observed that the gap is continuosly closed when U is lowered until the critical value U_{c1} is reached. In the inset of Fig.(4), we show the values of $\frac{4}{U^2+D^2}\int_{\infty}^{\infty} d\omega\ \omega^2 A(\omega)$ (squares), which represents the ratio of the second moment obtained within OCA and its exact value from Eq.(4), as a function of U and its deviation from the unity (solid line). It can be seen that OCA underestimates the second moment of the spectral function by $\sim 15\%$.

‡ With our notation the moments M_k are equal to the coefficients c_{k+1} defined in Ref. [31]

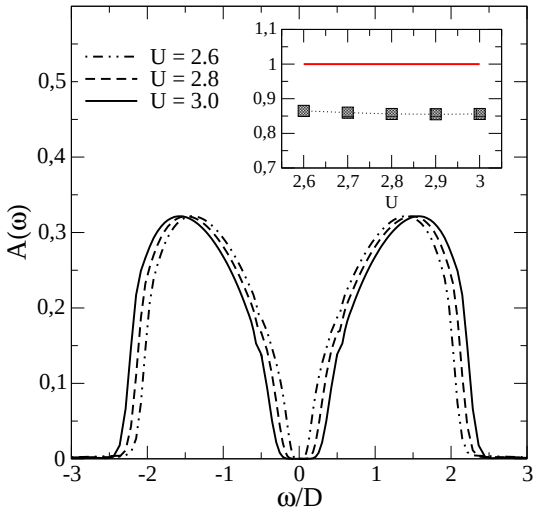

Figure 4. (Color online) Spectral density in the insulating region when decreasing the Coulomb repulsion from $U = 3$ to $U = 2.6$. The inset shows the ratio of the second moment obtained within OCA and its exact value from Eq.(4) (squares) as a function of U and its deviation from the unity (solid line).

Unfortunately, the center position and width of each Hubbard band enter in a combination within M_2 and we cannot know from this coefficient alone, if OCA underestimated the center position or width or even both. However, an underestimation in both quantities bring about a reduccion of the gap that gives rise to larger values of U_{c1} as compared with the exact CT-QMC ones.

3.2. Non-symmetric case

In this subsection, we compare the calculations done by OCA and CT-QMC for the one band Hubbard model on the Bethe lattice away from half-filling. We consider $2.5 < U < 5.0$ and the impurity level of the effective Anderson model at $\epsilon_d = -\frac{U}{2} + \Delta\mu$, with $\Delta\mu$=-1.0 and $\beta = 60$.

In Fig. 5, the spectral densities calculated by OCA for different values of U are shown. One may see that for the smallest value of U, the system is metallic with a large quasiparticle resonance that overlaps with the upper Hubbard band giving rise to large charge fluctuations pertaining to a mixed valence regime. In the other extreme, for the largest value of U, the systems is an insulator with the Hubbard bands located symmetrically with respect to $\Delta\mu$. The value of the gap in this case is of the order of $2D$. In order to be able to describe accurately solutions with large gaps, we implemented a three-centered logarithmic mesh.

By integrating $A(\omega)$ weigthed by the Fermi function for the corresponding temperature, we obtained the local occupancies in a very good agreement with the CT-QMC ones. It is not obvious that this quantity can be correctly evaluated within approximate analytical solvers. Hence, the fact that it is captured within OCA is important for the applicability of the method to non-symmetric cases.

In the inset of Fig.5 we show $A(\omega = 0)$ as a function of U in comparison with CT-QMC. One sees that both the OCA and CT-QMC indicate that the system turns an insulator for $U \geq 4.5$. For this level of doping there is no coexistence region and the OCA critical value U_c agrees with the CT-QMC one within a 5%.

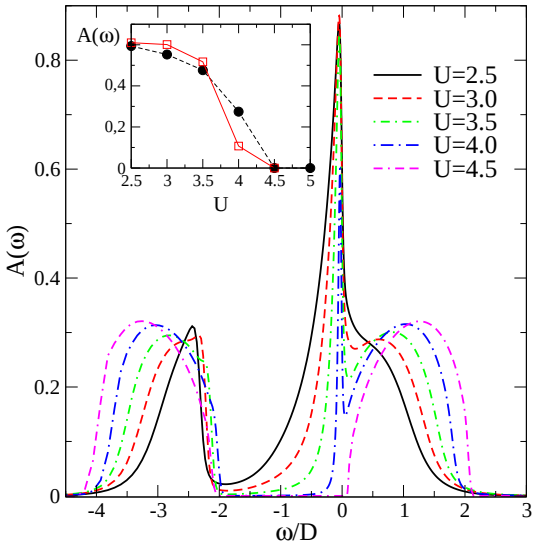

Figure 5. (Color online) Spectral density $A(\omega)$ calculated by OCA for a non-symmetric case taking $2.5 < U < 5.0$ and an energy shift of -1.0 from the corresponding symmetric case for each value of U. The inverse temperature is $\beta = 60$. In the inset we show $A(\omega = 0)$ as a function of U. The CT-QMC (OCA) data are displayed with the solid (dashed) lines and empty (filled) symbols, respectively.

Overall, we show that OCA also gives a very reasonable description of the Mott metal-insulating transition for the Hubbard model away from half-filling.

4. Summary and conclusions

The self-consistent hybridization expansions in their different forms (NCA, OCA, symmetric finite-U NCA, etc) have been widely used not only in the context of the impurity problem, but also in the framework of DMFT applied both to different lattice models and realistic cases, describing strongly correlated materials from first-principles. However, to the best of our knowledge, a detailed and quantitative study of the Mott transition, one of the essential problems of strongly correlated systems, has not been carried out up to now with these kind of approximate techniques.

In this work, we asses the reliability of OCA impurity solver in the context of the DMFT method to describe the Mott metal-insulator for the one band Hubbard model in the Bethe lattice at half-filling within DMFT. We present the temperature-local repulsion U phase diagram in comparison with the numerically exact CT-QMC. We show that OCA can provide a very good quantitative description of the metal-insulator transition of the present model. We obtain the metal-to-insulator transition, U_{c_2}, within an error of less than 0.5% while the insulator-to-metal U_{c_1} values are shifted to higher U

(about a 3%) with respect to the CT-QMC one. We explain the overestimation of U_{c_1} from an analysis of the second moment of the spectral density, M_2. We find that the expected theoretical value for M_2 is underestimated by OCA. Since M_2 is equal to the second moment of the spectral weight, we infer that the size of the gap in the insulating phase is also underestimated so that the Hubbard bands collapse for higher values of U than for CT-QMC.

Aside from the Mott transition itself, we confirm previous results[31, 32] regarding the better performance of OCA in the insulating phase than in the metallic one. The high-frequency sum rules for the imaginary part of $\Sigma(i\omega)$ are obtained reasonably well in both phases, with the deviation in the insulating case being a bit smaller than in the metallic one. On the other hand, in the small frequency region the correlations are overestimated in the metallic case. This effect is also apparent in the value of the quasiparticle weigth that is underestimated by OCA, specially far away from the transition. This overestimation of the correlations in the metallic phase does not imply that OCA favors the insulating state, as has been previously stated in Ref. [32], since we show the transition U is well reproduced, especially the U_{c_2} values. Furthermore, we show that the gap of the insulating phase is underestimated by OCA.

Finally, we study the perfomance of OCA for a non-symmetric case obtaining an overall reasonable agreement with CT-QMC, and a very similar critical value of U for the Mott transition at the considered temperature. The study of non-symmetric cases are particularly relevant for applications to real materials.

Despite the above mentioned deviations of OCA from exacts results, we are not aware of any other approximated technique yielding a phase-diagram with this level of agreement with numerically-exact many-body methods.

5. Acknowledgments

This work was partially supported by CONICET, PIP 00273 and 01060 and MINCYT-ANPCyT, program ECOS-MINCyT France-Argentina (project A13E04), PICT 1875 and R1776, Argentina.

6. Bibliography

[1] Metzner W and Vollhardt D, 1964 *Phys. Rev. Lett.* **62**, 324
[2] Georges A, Kotliar G, Krauth W, and Rozenberg M J, 1996 *Rev. Mod. Phys.* **68** 13
[3] Kotliar G, Savrasov S Y, Haule K, Oudovenko V S, Parcollet O, and Marianetti C A, 2006 *Rev. Mod. Phys.* **78**, 865
[4] Anderson P W, 1961 *Phys. Rev.* **124**, 41.
[5] Hirsch J E and Fye R M, 1986 *Phys. Rev. Lett.* **56** 2521.
[6] Werner P, Comanac A, de Medici L, Troyer M, and Millis A J, 2006 *Phys. Rev. Lett.* **97**, 076405 ; 2007 Haule K, *Phys. Rev. B* **75**, 155113.

[7] Wilson K G, 1975 *Rev. Mod. Phys.* **47**, 773 ; 2008 Bulla R, Costi T A, and Pruschke T, *Rev. Mod. Phys.* **80**, 395.

[8] Bulla R, Costi T A, and Vollhardt D, 2001 *Phys. Rev. B* **64**, 045103.

[9] Weichselbaum A, 2012 Annals of Physics **327**, 2972.

[10] Gull E, Millis A J, Lichtenstein A I, Rubtsov A N, Troyer M, and Werner P, 2011 *Rev. Mod. Phys.* **83**, 349.

[11] Stadler K M, Weichselbaum A, Yin Z P, von Delft J, and Kotliar G, arXiv:1503.06467.

[12] Pruschke T and Bulla R, 2005 *Eur. Phys. J. B.* **44** 217.

[13] Logan D E, Eastwood M P, and Tusch M A, 1998 *J. Phys.: Condens. Matter* **10**, 2673; Dickens N L and Logan D E, 2001 *J. Phys.: Condens. Matter* **13**, 4505; Smith V E, Logan D E, and Krishnamurthy H R, 2003 *Eur. Phys. J. B* **32**, 49; Vidhyadhiraja N S, Smith V E, and Logan D E, 2003 *J. Phys.: Condens. Matter* **15**, 4045.

[14] Muller-Hartmann E, 1989 *Int. J. Mod. Phys.* **3**, 2169; Vollhardt D, 1991 *Physica B* **169**, 277.

[15] Caffarel M and Krauth W, 1994 *Phys. Rev. Lett.* **72**, 1545.

[16] Lechermann F et al. 2007 *Phys Rev. B* **76** 155102.

[17] Kroha J and Wölfle P, 2005 *J. Phys. Soc. Jpn.* **74**, 16-26.

[18] Bickers N E, 1987 *Rev. Mod. Phys.* **59**, 845; Coleman P, 1983 *Phys. Rev. B* **29**, 3035.
1996 *Phys. Rev. B,* **54**, 6494; *ibid.*, 1997 **55**, 12 594; Han J E *et al.*, 1997 *Phys. Rev. Lett.* **78** 939; Vildosola V L, Alouani M and Llois A M, 2005 *Phys. Rev. B* **71**, 184420; Roura-Bas P, Vildosola V and Llois A M, 2007 *Phys. Rev. B* **75**, 195129.
Hettler M H, Kroha J, and Hershfield S, 1994 P*hys. Rev. Lett.* **73** 1967; Roura-Bas P, 2010 *Phys. Rev. B* **81**, 155327.

[19] Pruschke Th and Grewe N, 1989 *Z. Phys. B - Condensed Matter* **74**, 439.

[20] Haule K, Kirchner S, Kroha J, and Wölfle P, 2001 *Phys. Rev. B* **64**, 155111.

[21] Tosi L, Roura-Bas P, Llois A M, and Manuel L O, 2011 *Phys. Rev. B* **83**, 073301.

[22] Jacob D, Haule K and Kotliar G, 2009 *Phys. Rev. Lett.* **103**, 016803.

[23] Haule K, Yee C -H, and Kim K, 2010 *Phys. Rev. B* **81**, 195107.

[24] Schmitt S, 2010 *Phys. Rev. B* **82**, 155126.

[25] Yin Q, Kutepov A, Haule K, and Kotliar G, 2011 *Phys. Rev. B* **84**, 195111; Choi H Ch, Min B I, Shim J H, Haule K, and Kotliar G, 2012 Phys. Rev. Lett. 108, 016402.

[26] Kotliar G, Savrasov S Y, Haule K, Oudovenko V S, Parcollet O, and Marianetti C A, 2006 *Rev. Mod. Phys.* **78**, 865.

[27] Schmitt S, Grewe N, and Jabben T, 2012 *Phys. Rev. B* **85**, 024404.

[28] Grewe N, Schmitt S, Jabben T, and Anders F B, 2008 *J. Phys.: Condens. Matter* **20**, 365217.

[29] Grewe N, Jabben T, and Schmitt S, 2009 *Eur. Phys. J. B* **68**, 23.

[30] Schmitt S, Jabben T, and Grewe N, 2009 *Phys. Rev. B* **80**, 235130.

[31] Rüegg A, Gull E, Fiete G A, and Millis A J, 2013 *Phys. Rev. B* **87**, 075124.

[32] Rüegg A, Hung H -H, Gull E, and Fiete G A, 2014 *Phys. Rev. B* **89**, 085122.

[33] Mott N F, 1968 *Rev. Mod. Phys.* **40**, 677

[34] Rozenberg M J, Chitra R, and Kotliar G, 1999 *Phys. Rev. Lett.* **83**, 3498.

[35] Joo J and Oudovenko V, 2001 *Phys. Rev. B* **64** 193102.

[36] Blm̈er N, *Metal-Insulator Transition and Optical Conductivity in High Dimensions*, Shaker Verlag, Aachen 2003.

[37] Caffarel M and Krauth W, 1994 *Phys. Rev. Lett.* **72** 1545.

[38] Rozenberg M J, Moeller G, and Kotliar G, 1994 *Mod. Phys. Lett. B* **8** 535 1994.

[39] Tong N, Shen S, and Pu F, 2001 *Phys. Rev. B* **64** 235109 2001.

[40] Ferrero M and Parcollet O, "Triqs: a toolkit for research in interacting quantum systems", http://ipht.cea.fr/triqs.

[41] Parcollet O, Ferrero M, Ayral T, Hafermann H, Krivenko I, Messio L, and Seth P, arXiv:1504.01952.

[42] Hettler M H, Kroha J, and Hershfield S, 1994 *Phys. Rev. Lett.* **73** 1967 1994.

[43] Liebsch A, 2004 *Phys. Rev. B* **70** 165103 2004.

[44] The rule $\Sigma_1 = -U^2/4$ follows from the spinless model analyzed in Ref.[31] (with a minus missed sign).